

# Radical Pair Mechanism and the role of Chirality-Induced Spin Selectivity during Planaria Regeneration: Effect of Weak Magnetic Field on ROS levels

Yash Tiwari, Parul Raghuvanshi and Vishvendra Singh Poonia

## 1. Effect of the recombination rates

### (a) Singlet initiated when $\chi=0$

The initial state for the following case of two radicals

$$|\psi_{In} \rangle = \cos\left(\frac{\chi}{2}\right) |S \rangle + \sin\left(\frac{\chi}{2}\right) |T_0 \rangle \quad (1)$$

$$P_{In} = |\psi_{In} \rangle \langle \psi_{In}| = \begin{bmatrix} 0 & 0 & 0 & 0 \\ 0 & 0.5(1 + \sin \chi) & -0.5 \cos \chi & 0 \\ 0 & -0.5 \cos \chi & 0.5(1 - \sin \chi) & 0 \\ 0 & 0 & 0 & 0 \end{bmatrix} \quad (2)$$

The recombination operator is the following.

$$|\psi_S \rangle = \cos\left(\frac{\chi}{2}\right) |S \rangle - \sin\left(\frac{\chi}{2}\right) |T_o \rangle \quad (3)$$

$$P_S = |\psi_S \rangle \langle \psi_S| = \begin{bmatrix} 0 & 0 & 0 & 0 \\ 0 & 0.5(1 - \sin \chi) & -0.5 \cos \chi & 0 \\ 0 & -0.5 \cos \chi & 0.5(1 + \sin \chi) & 0 \\ 0 & 0 & 0 & 0 \end{bmatrix} \quad (4)$$

$$|\psi_{T_o} \rangle = \sin\left(\frac{\chi}{2}\right) |S \rangle + \cos\left(\frac{\chi}{2}\right) |T_o \rangle \quad (5)$$

$$P_{T_o} = |\psi_{T_o} \rangle \langle \psi_{T_o}| = \begin{bmatrix} 0 & 0 & 0 & 0 \\ 0 & 0.5(1 + \sin \chi) & 0.5 \cos \chi & 0 \\ 0 & 0.5 \cos \chi & 0.5(1 - \sin \chi) & 0 \\ 0 & 0 & 0 & 0 \end{bmatrix} \quad (6)$$

$$P_{T+} = \begin{bmatrix} 1 & 0 & 0 & 0 \\ 0 & 0 & 0 & 0 \\ 0 & 0 & 0 & 0 \\ 0 & 0 & 0 & 0 \end{bmatrix} \quad P_{T-} = \begin{bmatrix} 0 & 0 & 0 & 0 \\ 0 & 0 & 0 & 0 \\ 0 & 0 & 0 & 0 \\ 0 & 0 & 0 & 1 - \sin \chi \end{bmatrix} \quad (7)$$

	$FAD^{\cdot-} TrpH^+$	$FADH^{\cdot-} O_2^{\cdot-}$
<b>Eq. 2 Initial state, CISS in formation and recombination Singlet initiated (when <math>\chi=0</math>)</b>	Fig 1	Fig 2
<b>Eq. 2 Initial state, CISS in the formation only Singlet initiated (when <math>\chi=0</math>)</b>	Fig 3	Fig 4
<b>Eq. 8 Initial state, CISS in formation and recombination Triplet initiated (when <math>\chi=0</math>)</b>		
<b>Eq. 8 Initial state, CISS in the formation only Triplet initiated (when <math>\chi=0</math>)</b>		

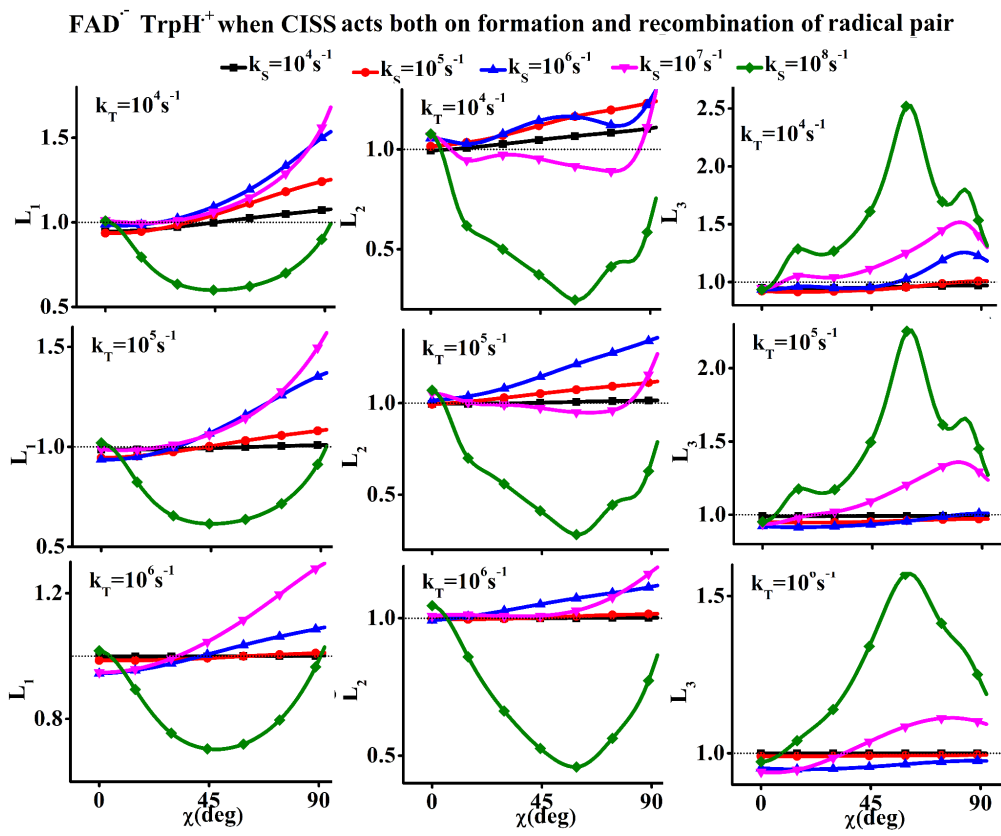


*Figure1:  $FAD^{\cdot-} TrpH^+$  when initial state is given by Eq. 2 when CISS is present in both formation and recombination of radical pair*

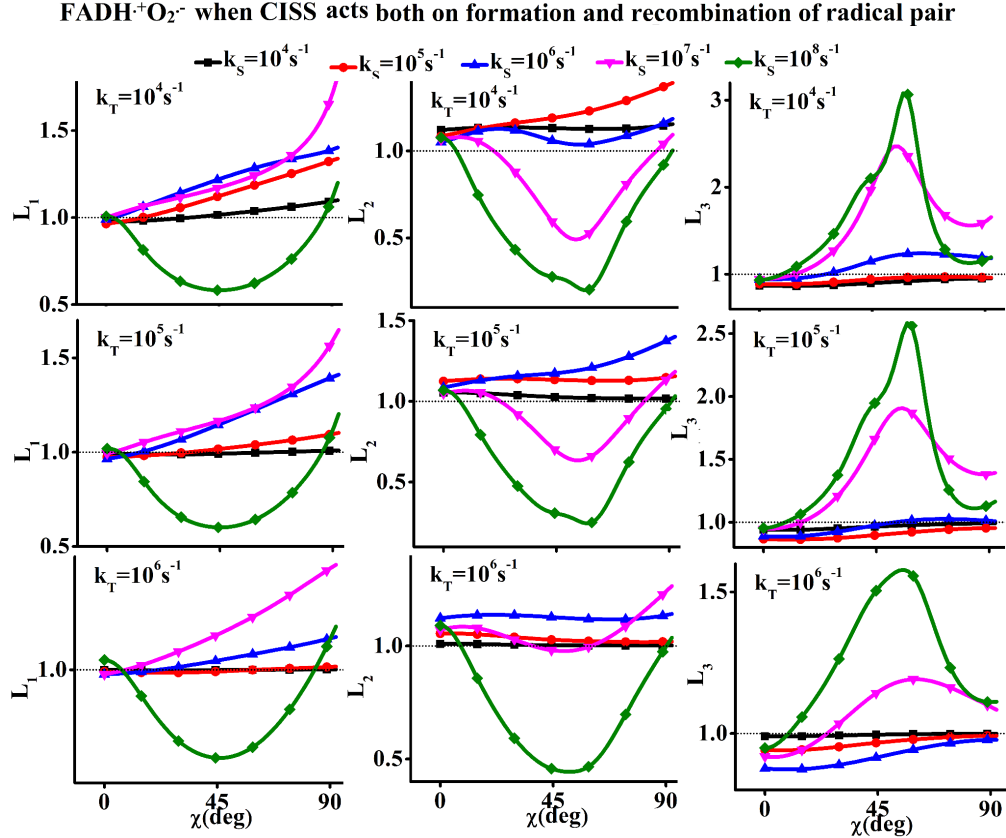


*Figure2:  $FADH^+ O_2^{\cdot-}$  when initial state is given by Eq. 2 when CISS is present in both formation and recombination of radical pair*

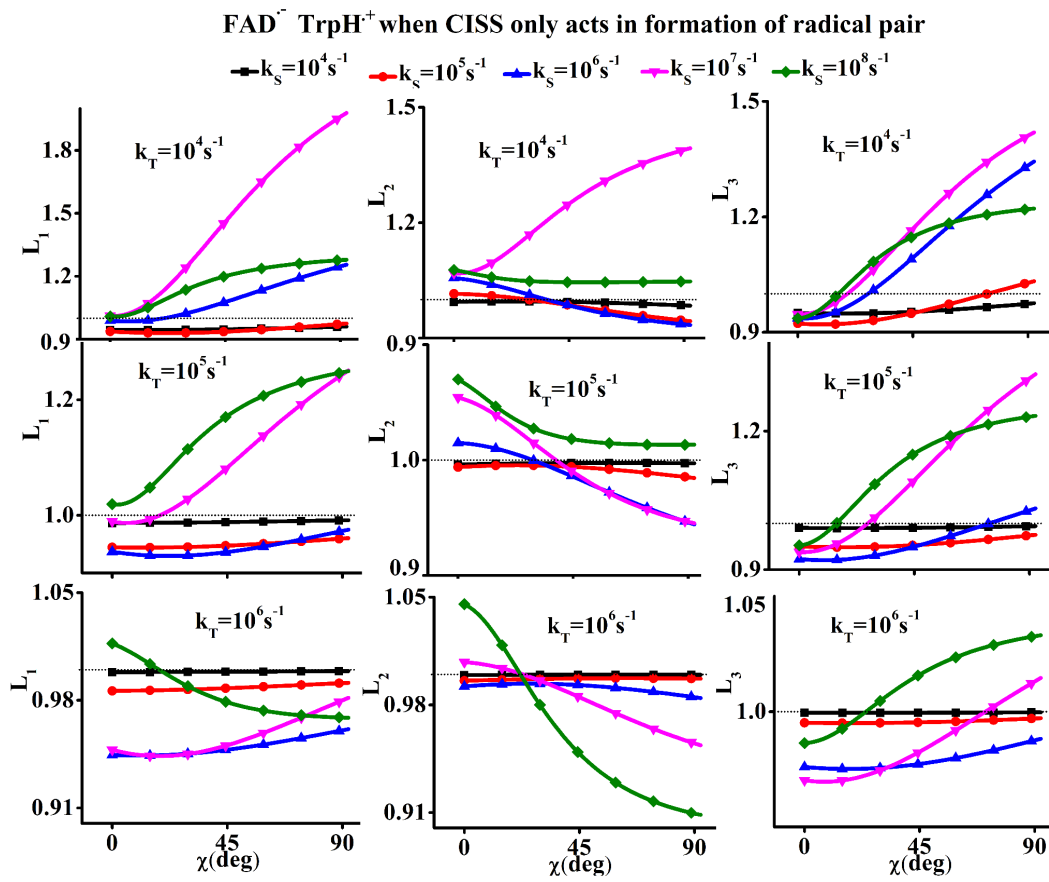


*Figure3: FAD<sup>-</sup> TrpH<sup>+</sup> when initial state is given by Eq. 2 when CISS is present in only in formation of radical pair*

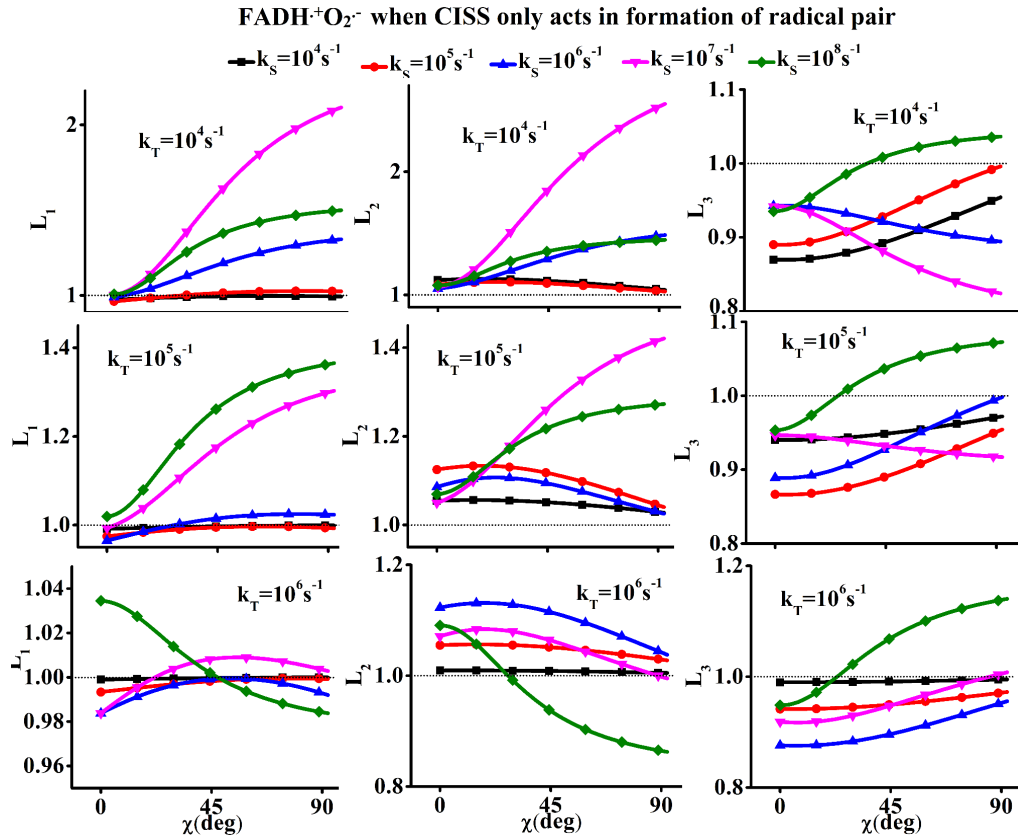


*Figure4: FADH<sup>+</sup> O<sub>2</sub><sup>-</sup> when initial state is given by Eq. 2 when CISS is present in only in formation of radical pair*

**(b) Triplet initiated when  $\chi = 0$**

The initial state for the following case of two radicals. Eq. (8) is normalized when used as the initial state.

$$P_{In} = P_T = P_{T0} + P_{T+} + P_{T-} \quad (8)$$

The recombination operator is the same as what is considered.

	$FAD^{\cdot-} TrpH^+$	$FADH^{\cdot-} O_2^{\cdot-}$
Eq. 2 Initial state, CISS in formation and recombination Singlet initiated (when $\chi = 0$ )	Fig 1	Fig 2
Eq. 2 Initial state, CISS in the formation only Singlet initiated (when $\chi = 0$ )	Fig 3	Fig 4
Eq. 8 Initial state, CISS in formation and recombination Triplet initiated (when $\chi = 0$ )	Fig 5	Fig 6
Eq. 8 Initial state, CISS in the formation only Triplet initiated (when $\chi = 0$ )	Fig 7	Fig 8

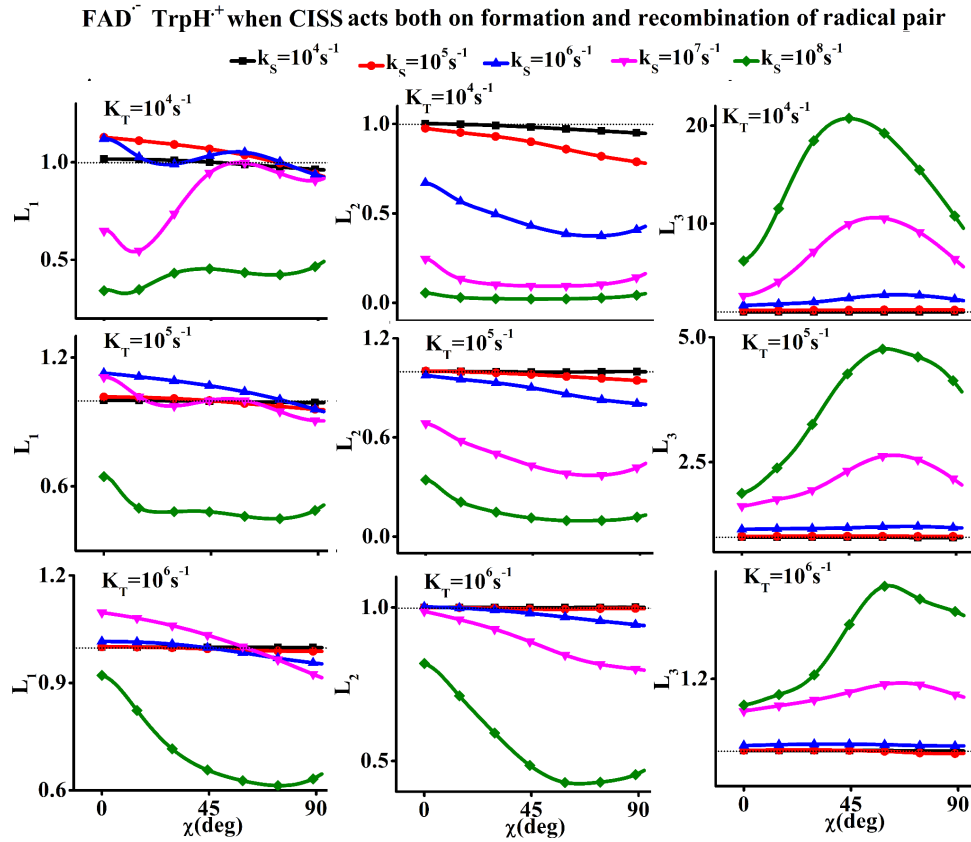


**Figure5:**  $FAD^{\cdot-} TrpH^+$  when intial state is given by Eq. 8 when CISS is present

*in both formation and recombination of radical pair*

**FADH<sup>•</sup>O<sub>2</sub><sup>-</sup> when CISS acts both on formation and recombination of radical pair**

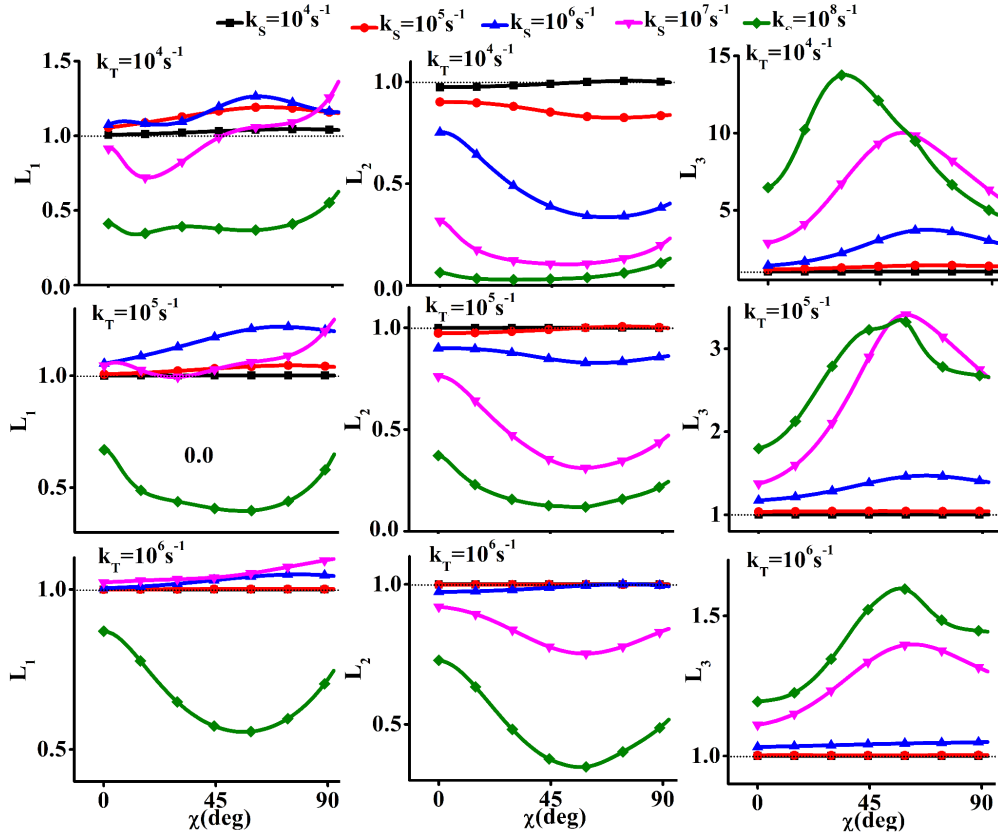


**Figure6:** FADH<sup>•</sup>O<sub>2</sub><sup>-</sup> when initial state is given by Eq. 8 when CISS is present  
*in both formation and recombination of radical pair*

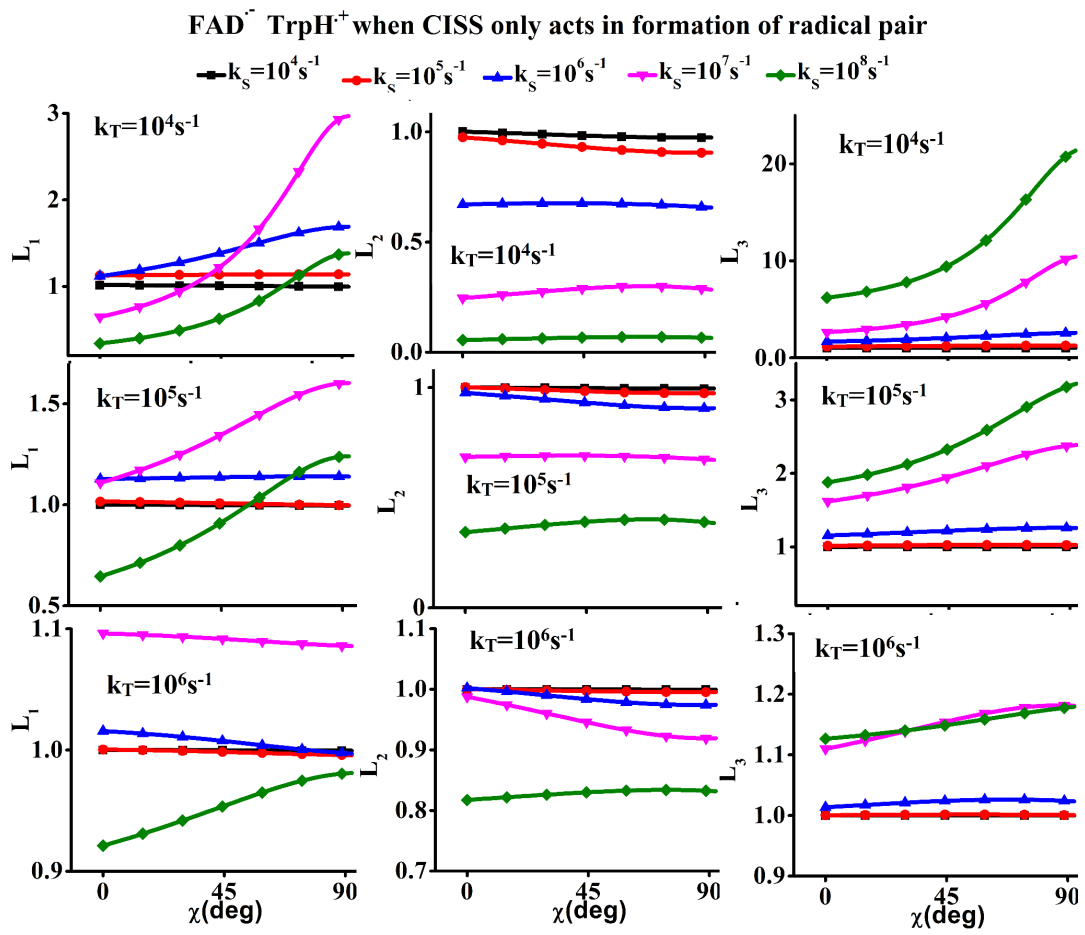


*Figure7:  $FAD^{\cdot-} TrpH^+$  when initial state is given by Eq. 8 when CISS is present only in formation of radical pair*

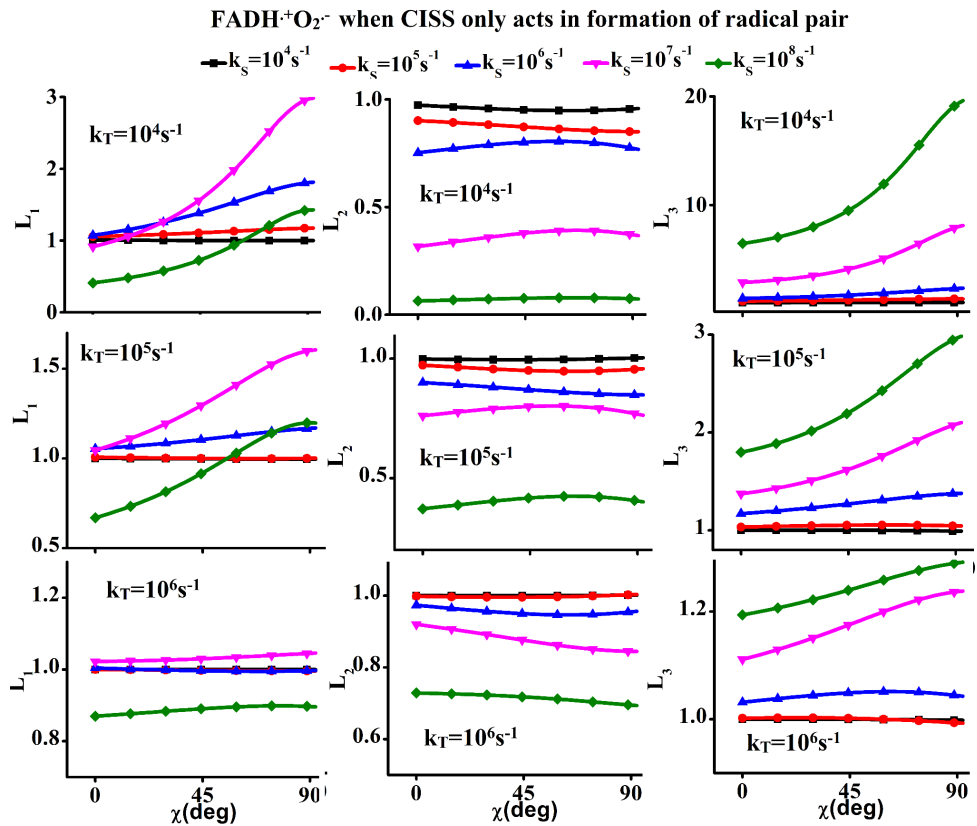


*Figure8:  $FADH^+ O_2^{\cdot-}$  when initial state is given by Eq. 8 when CISS is present only in formation of radical pair*

## 2. Peaks at 500 $\mu$ T for anisotropic hyperfine interaction

	$FAD^{\cdot-} TrpH^+$	$FADH^{\cdot-} O_2^{\cdot-}$
<b>Eq. 2 Initial state, CISS in formation and recombination at <math>\chi = \frac{\pi}{2}</math></b>	Fig9 (Just at $\chi = \frac{\pi}{2}$ at $k_S=10^7 s^{-1}$ and $k_T=10^4 s^{-1}$ )	

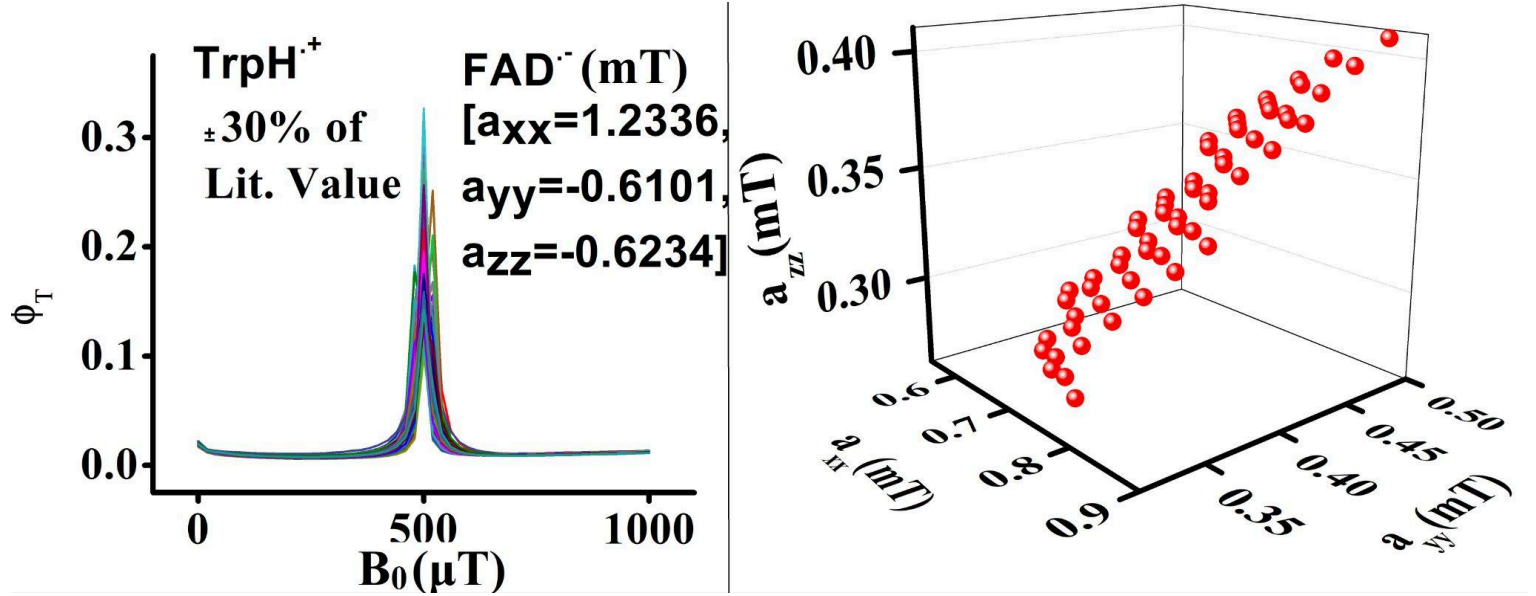


**Figure 9:** (Left)  $\Phi_T$  for  $FAD^{\cdot-} TrpH^+$  where the hyperfine value of  $TrpH^+$  is varied by  $\pm 30\%$  of the literature value. Here  $\Phi_T(500 \mu T) > 10 \cdot \Phi_T(45 \mu T)$ . This is done for the case when  $D=0$  mT,  $J=0$  mT, and  $\chi = \frac{\pi}{2}$  at  $k_S=10^7 s^{-1}$  and  $k_T=10^4 s^{-1}$ . Moreover, this corresponds to the case when CISS acts both in the formation and recombination of radical pairs. (Right) Each red point corresponds to the hyperfine tensor of  $TrpH^+$  with corresponding  $[a_{xx}, a_{yy}, a_{zz}]$  where  $\Phi_T(500 \mu T) > 10 \cdot \Phi_T(45 \mu T)$

In Fig.9 (Left), we demonstrate that it is indeed possible to observe distinctive peaks at  $500 \mu T$  at  $k_S=10^7 s^{-1}$  and  $k_T=10^4 s^{-1}$  and  $D=0$  mT. However, we have deviated from the established literature values for the hyperfine tensor to achieve this. This allows some flexibility due to potential structural vibrations or folding that might occur in a biological medium and alter the hyperfine values. Considering the scenario where  $FAD^{\cdot-} TrpH^+$  is involved, with the initial state as  $\chi = \frac{|S\rangle + |T_0\rangle}{\sqrt{2}}$  at  $\chi = \frac{\pi}{2}$ , and with CISS contributing to both the formation and recombination of the radical pair, we calculated Fig.9 (Left). For simplicity of analysis, we adhered to the literature values  $FAD^{\cdot-}$ ; however, we adjusted the anisotropic hyperfine component  $TrpH^+$ , varying it by  $\pm 30\%$  of the established literature value to explore the effects of such variations. Fig. 9(Right) consists of a scatter plot where each red point corresponds to the hyperfine tensor  $TrpH^+$  with corresponding  $[a_{xx}, a_{yy}, a_{zz}]$  where  $\Phi_T(500 \mu T) > 10 \cdot \Phi_T(45 \mu T)$ .



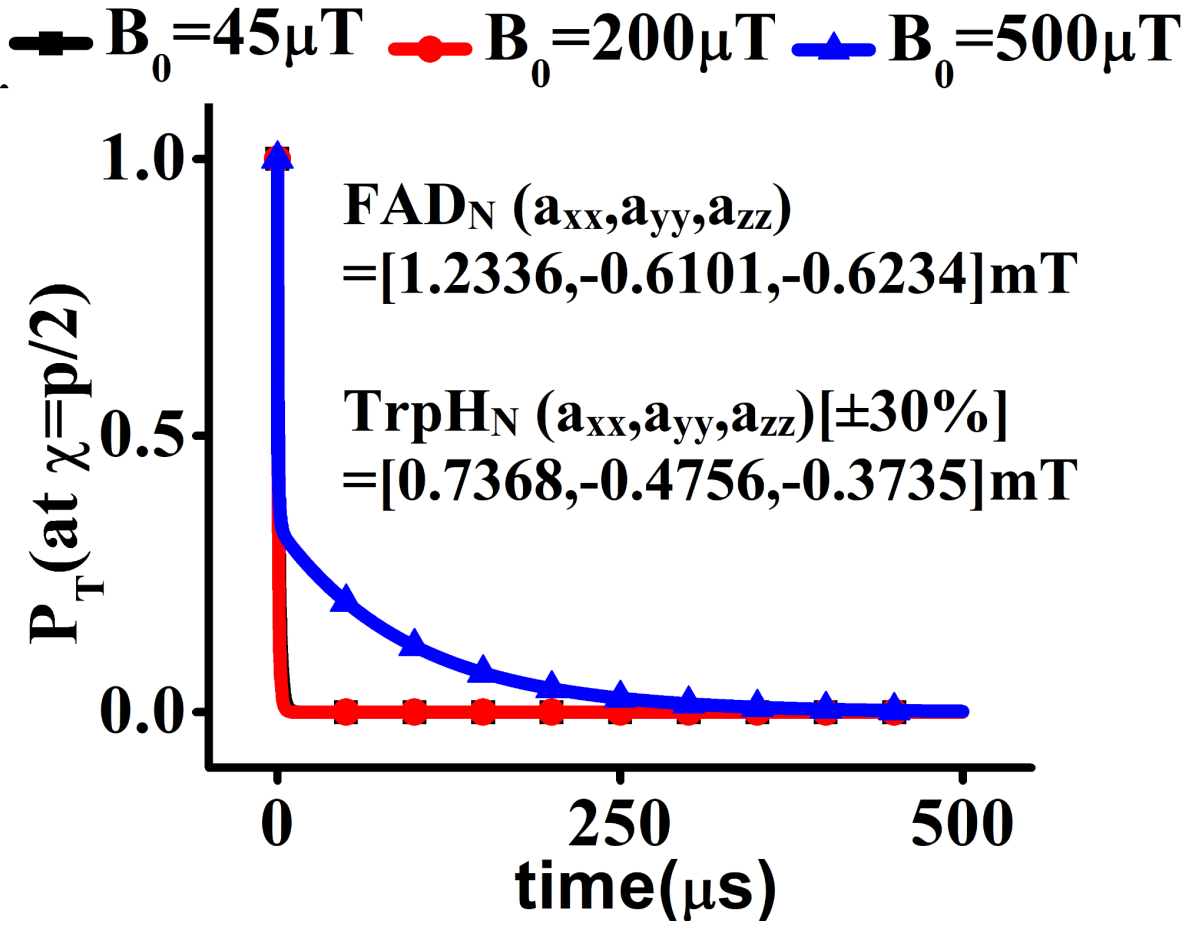


**Figure 10:**  $P_T$  for  $FAD^{\cdot-} TrpH^+$  where the hyperfine tensor value of  $TrpH^+$  is varied by  $\pm 30\%$  of the literature value while  $FAD^{\cdot-}$  hyperfine tensor values are from literature. This is done for the case when  $D=0\text{mT}$ ,  $J=0\text{mT}$ , and  $\chi = \frac{\pi}{2}$  at  $k_S=10^7\text{s}^{-1}$  and  $k_T=10^4\text{s}^{-1}$ . Moreover, this corresponds to the case when CISS acts both in the formation and recombination of radical pairs.

In Fig.10, we plotted  $P_T$  (Eq.8), for  $FAD^{\cdot-} TrpH^+$  where the hyperfine tensor value  $TrpH^+$  is varied by  $\pm 30\%$  of the literature value (exact value in Fig. 10) while  $FAD^{\cdot-}$  hyperfine tensor values are from the literature. This is done for the case when  $D=0\text{mT}$ ,  $J=0\text{mT}$ , and  $\chi = \frac{\pi}{2}$  at  $k_S=10^7\text{s}^{-1}$  and  $k_T=10^4\text{s}^{-1}$ . We observe that the lifetime  $P_T$  is much greater at  $500\mu\text{T}$  compared to  $200\mu\text{T}$  and  $45\mu\text{T}$ , illustrating the reason for the peak as observed in Figure 9: (Left).

### 3. Hyperfine Interaction

The hyperfine tensors used in our study are based on the work by Hiscock et al. [1-2]. The  $FAD^{\cdot-} TrpH^+$  molecules are drawn in Fig. 11. The nuclei considered in our simulations on each molecule are marked in red. The isotropic hyperfine values of labeled nuclei are given below.

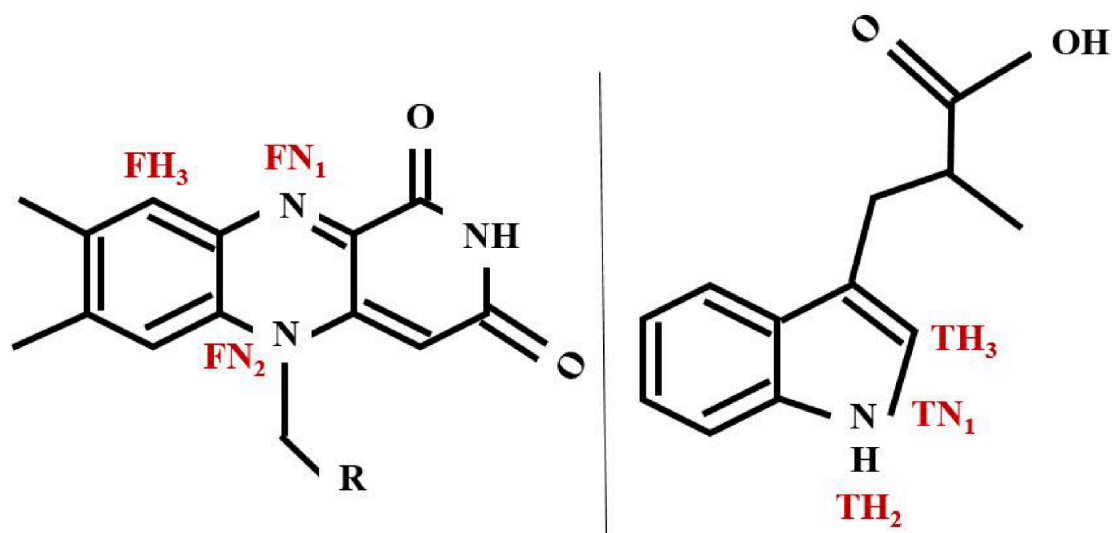


**Figure 11:** (a)  $FAD^{\bullet-}$  molecule and (b)  $TrpH^+$  molecule. The nuclei marked in red are considered in our calculation. The first letter corresponds to the molecule type (F- $FAD^{\bullet-}$  and T- $TrpH^+$ ), and the second letter corresponds to the nuclei type (N-nitrogen and H-hydrogen)

**Table 1:** Hyperfine interaction in mT for  $FAD^{\bullet-}$  ( $FN_1$ ,  $FN_2$ ,  $FH_3$ ) and  $TrpH^+$  ( $TN_1$ ,  $TH_2$ ,  $TH_3$ )

$FN_1$	$FN_2$	$FH_3$	$TN_1$	$TH_2$	$TH_3$
0.5233	0.1887	-0.3872	0.3215	-0.5983	-0.2780

Similarly, the structure  $FADH^{\bullet-} O_2^{\bullet-}$  is given in Fig. 12, followed by its hyperfine distribution [3].

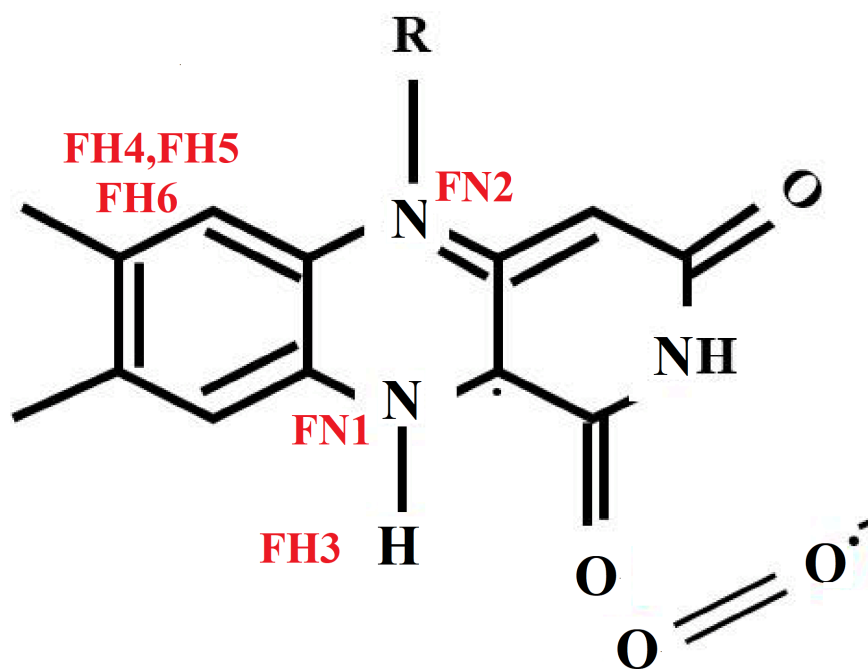


**Figure 12:**  $FADH^{\bullet-} O_2^{\bullet-}$  molecule. The nuclei marked in red are considered in our calculation.

**Table 2:** Hyperfine interaction in mT for FADH<sup>•</sup> ( $FN_1, FN_2, FH_3, FH_4, FH_5, FH_6$ )

$FN_1$	$FN_2$	$FH_3$	$FH_4$	$FH_5$	$FH_6$
0.4313	0.2506	-0.8029	0.3737	0.3845	0.0080

**References**

[1] H. Hiscock, “Long-lived spin coherence in radical pair compass magnetoreception,” Ph.D. dissertation, University of Oxford, 2018.

[2] H. G. Hiscock, S. Worster, D. R. Kattnig, C. Steers, Y. Jin, D. E. Manolopoulos, H. Mouritsen, and P. J. Hore, “The quantum needle of the avian magnetic compass,” *Proceedings of the National Academy of Sciences*, vol. 113, no. 17, pp. 4634--4639, 2016, National Acad Sciences.

[3] A. A. Lee, J. C. S. Lau, H. J. Hogben, T. Biskup, D. R. Kattnig, and P. J. Hore, “Alternative radical pairs for cryptochrome-based magnetoreception,” *Journal of The Royal Society Interface*, vol. 11, no. 95, pp. 20131063, 2014, The Royal Society.